

## Measuring rock glacier surface deformation using SAR interferometry

L.W. Kenyi

*Institute for Digital Image Processing, Joanneum Research, Graz, Austria*

V. Kaufmann

*Institute of Geodesy, Graz University of Technology, Austria*

**ABSTRACT:** The detection and quantification of surface deformation of an active rock glacier using the differential SAR interferometry technique is presented. An average deformation rate of  $-6$  mm/35 days in the radar line-of-sight in the summer of 1992 was estimated. The maximum deformation rate was located at the upper part of the rock glacier and amounts to  $-18$  mm/35 days. In contrast, at the snout of the rock glacier the deformation rate was only around  $-10$  mm/35 days. The spatial distribution of the surface deformation in the D-InSAR displacement map is smooth and supports the idea that ice is the stress transferring medium in rock glaciers.

### 1 INTRODUCTION

In a Synthetic Aperture Radar (SAR) system, both the amplitude and the phase of the backscattered echoes are normally recorded. As the phase of a single SAR image is of no use however, conventionally only the amplitude or intensity image is usually provided to the end users. The phase difference of two backscattered SAR echoes of the same ground surface area taken at slightly different view angles can however be utilized to generate digital elevation model (DEM) of the imaged terrain (Prati et al. 1992, Zebker et al. 1994, Kenyi & Raggam 1996). This technique is known as SAR interferometry (InSAR) and can be extended to differential SAR interferometry (D-InSAR) to detect small surface changes in the order of few centimeters (Gabriel et al. 1989). Although the D-InSAR method has been shown to successfully detect surface displacement in the radar line-of-sight caused by earthquakes (Massonet et al. 1993), or mass movements in the alpine and arctic terrain (Rott & Siegel 1999, Wang & Li 1999), additional investigations in high mountain environments have yet to be performed.

A number of questions related to the properties of rock glaciers, which are creep phenomena of discontinuous mountain permafrost (Barsch 1996), and the imaging geometry of the SAR sensor remain to be answered. These include (1) the relatively small sizes of alpine rock glaciers in comparison to the SAR pixel resolution, (2) the rough surface topography composed of debris and rocks, (3) the perennial snow patches and snow cover in the areas of interest, (4) the rather small flow velocities of active rock glaciers in the range of centimetres to a few metres per annum, (5) the look angle of the SAR sensor, and (6) the geometric and temporal baselines requirements for successful D-InSAR data sets.

In this paper, the detection and quantification of surface deformation of an actively creeping, alpine rock

glaciers using InSAR data is reported. Additionally, the prerequisites to perform such an analysis in the alpine region are given. A comparison of the D-InSAR results with available geodetic and photogrammetric measurements is presented.

In Section 2, the principles of D-InSAR are described in detail and in Section 3 the description of the test area, the compiled SAR data, and the interferometric processing procedure are presented. Discussion and the quantitative analysis of the achieved results are presented in Section 4. The conclusions and the scope for future work are given in Section 5.

### 2 PRINCIPLES OF D-INSAR

The difference of two interferograms can be used to measure small surface changes over large areas at a scale in the order of centimetres (Gabriel et al. 1989). The interferometric phase is sensitive to both surface topography and coherent displacement along the SAR look vector occurring between the acquisition of the interferometric image pair. The basic idea in the differential technique is to remove the topography related phase whilst the remaining phase provides the displacement. In practice however, noise and path propagation related phases have to be taken into consideration. Details of the D-InSAR technique can be found in the literature (Gabriel et al. 1989, Massonet et al. 1993, and Zebker et al. 1994).

The phase  $\phi$  measured by a repeat orbit InSAR system can be expressed as in Equation 1 (see Zebker et al. 1994):

$$\phi = \frac{4\pi}{\lambda} \Delta r \quad (1)$$

where  $\Delta r$  is the difference in range and includes components other than that contributed by the topography.

These components are summarised in Equation 2 (*see Wegmueller & Strozzi 1998*):

$$\begin{aligned} \phi = & \phi_{\text{terrain}} + \phi_{\text{displacement}} + \phi_{\text{atmosphere}} \\ & + \phi_{\text{noise}} + \phi_{\text{processing}} \end{aligned} \quad (2)$$

Equation 2 implies that to obtain the displacement phase, we need to estimate the other phase contributions. The phase due to noise comprises three components, thermal noise and baseline and temporal decorrelation. Thermal noise can be rejected because the signal-to-noise ratio of the ERS sensor in this case is designed to be maximum. Baseline decorrelation can be reduced by spectral shift filtering if the normal baseline component is greater than the ERS optimal value (200 m). Temporal decorrelation is inherent and can be minimized by selection of image pairs of smaller temporal baselines. Other factors which must be taken into account are the phase due to processing errors, atmospheric displacement and the topographical phase. The phase due to processing errors is important but can also be considered as noise in the data. Similarly, the atmospheric displacement can be ignored in this case as the area of investigation is smaller than the spatial scale of the tropospheric variation. The most influential factor is the phase due to topography, which can either be estimated from a DEM or from another interferogram of a relatively large normal baseline component. The remaining phase after the removal of the unwanted phase components can be considered as a consequence of displacement and is expressed as in Equation 3, (*see Zebker et al. 1994*):

$$\phi_{\text{displacement}} = \frac{4\pi}{\lambda} \rho \quad (3)$$

For the ERS SAR sensor, a one cycle phase shift will imply a displacement of 28.3 mm in the SAR slant range direction.

### 3 DATA AND PROCESSING

#### 3.1 Test area and data compilation

The Doesen rock glacier is located in the inner Doesen Valley within the Austrian Hohe Tauern National Park in the province of Carinthia. Its geographic coordinates are approximately 46°59'N and 13°17'E. It is one of two permafrost study test sites in Austria under detailed investigation using a number of different methods (*see also Rott & Siegel 1999*).

The glacially shaped, west-east oriented inner Doesen Valley covers an area of about 3 km<sup>2</sup> and stretches from 2200 m to 3086 m above sea level, (Figure 1b).

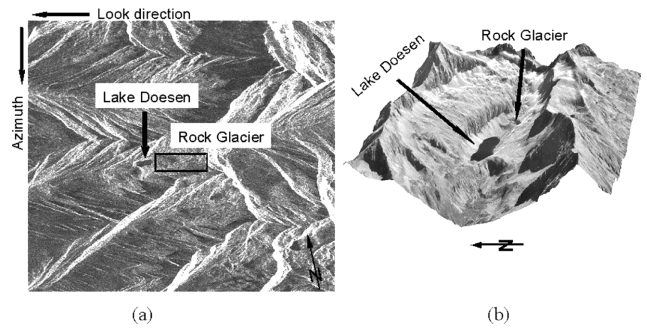


Figure 1. (a) ERS SAR sub amplitude image of the test area and (b) aerial photo perspective view from West direction of the area of interest. It is evident that the terrain is rugged and the relief energy is very high.

It consists of crystalline rocks, predominantly granitic gneiss, and is characterised by diversified glacial and pre-glacial morphology containing various talus features, the majority formed by permafrost processes. The centre of the study area is occupied by the active Doesen rock glacier (length 900 m, area 0.4 km<sup>2</sup>). The mean annual air temperature is  $-2^{\circ}\text{C}$  at 2550 m and the annual precipitation amounts to about 2000 mm at the same altitude, thus enabling areas with and without permafrost to be studied. Most of the area is free of compact vegetation cover. Under the bouldery surface at the foot of the north-facing slopes, including Doesen rock glacier, permafrost extends down to approximately 2270 m (snout of Doesen rock glacier at 2350 m). According to geophysical soundings (seismic, electromagnetic and ground-penetrating radar measurements), the mean thickness of the rock glacier is likely to be in the range of 30–40 m. The total volume of the rock glacier is estimated at  $15 \times 10^6 \text{ m}^3$ . Detailed information on high-mountain permafrost in the Austrian Alps and on the Doesen rock glacier in particular can be found in Lieb (1998). Since 1995 geodetic and photogrammetric measurements have been carried out at the Doesen rock glacier to study the spatial and temporal variations of the rock glacier surface. A maximum mean horizontal flow velocity of about 30 cm/annum was measured in the lower central part of the Doesen rock glacier (Kaufmann 1998).

For the InSAR data, five ERS-1/2 SAR single look complex (SLC) image data sets acquired during the period 1992 to 1997 over the Hohe Tauern range were compiled. In the selection of the data sets the weather conditions around the time of acquisition were taken into account to minimize atmospheric effects. The geodetic field campaigns and aerial photographs (*see Figure 1b*) have shown the Doesen rock glacier to be almost snow free during the period August–September, except for some minor areas with perennial snow patches. The selection of the interferometric image pairs was thus concentrated on this season of the year.

Table 1. Compiled ERS-1/2 data sets.

Orbit number	Acquisition date	Product type
05778 ERS-1	23.08.1992	SLCI*
06279 ERS-1	27.09.1992	SLCI
21152 ERS-1	01.08.1995	SLCI
31673 ERS-1	05.08.1997	SLCI
12000 ERS-2	06.08.1997	SLCI

\* SLCI stands for single look complex ERS SAR full scene product.

The orbit numbers of the selected scenes are listed in Table 1.

### 3.2 Data processing

For the generation of any D-InSAR products the classical interferometric processing chain must first be applied to the SLC image data. This involves: (1) the determination of shifts between the master image and the other slave images, (2) the resampling of the slave images to the raster geometry of the master image and (3) generation of the multi-looked InSAR products. We applied our own, in house developed, InSAR tools. The detailed description of the procedures can be found in Kenyi et al. (1996). After the co-registration, interferometric products from all possible combinations of the data sets listed in Table 1 were generated. The InSAR multi-looked was chosen as 5 looks and corresponds to about  $20 \times 20 \text{ m}^2$  ground pixel spacing. This is sufficient to allow the detection of the small scale Doesen rock glacier. The orbit combinations 06279-05778 and 12000-31673 showed the best coherence. The normal baseline component of the 12000-31673 orbit pair combination was very large however, at about 376 m, and the topographic phase was dominant. The normal baseline component of the 06279-05778 was only 7 m, which is perfect for D-InSAR application purposes.

Since one of the interferograms has an almost zero normal baseline component (7 m), its flat terrain filtered interferogram could be directly interpreted as the displacement phase. The test area however is characterised by very high relief and a rugged terrain. Even though the normal baseline component is very small, the relief effect is still present in the flattened interferogram. This point was checked by comparing the flattened interferogram with the simulated wrapped interferogram as shown in Figure 3. It was decided to apply the 2-pass D-InSAR (Wegmueller & Strozzi 1998) approach because of the availability of an accurate DEM of the test area. The estimation of the topographic phase from the ERS tandem orbit pair 12000-13673 was avoided mainly because of unwrapping errors due to the rugged terrain (layover and shadow areas) (Wegmueller & Strozzi 1998).

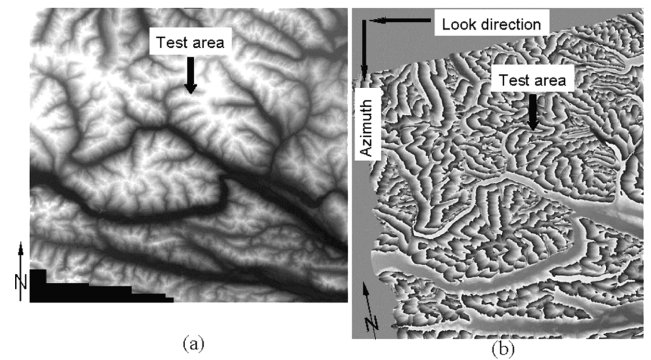


Figure 2. (a) The DEM used for the topographic phase simulation. (b) The simulated interferogram using imaging parameters of ERS-1 orbits 05578 and 06279. Only the wrapped version is presented here. For subtraction the absolute simulated interferogram was used.

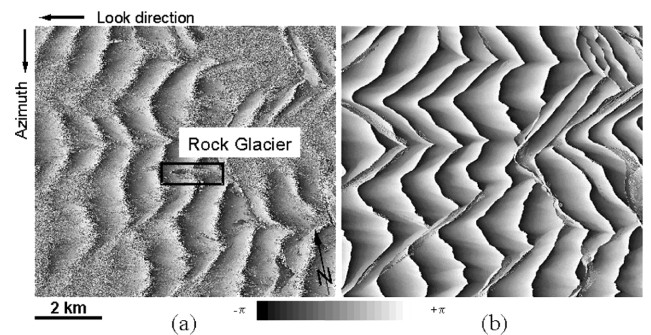


Figure 3. Comparison of the InSAR measured and simulated interferograms. (a) ERS InSAR measured and (b) DEM simulated. The interferometric multi-looked is 5 looks for both interferograms.

### 3.3 Simulation of interferogram

Using the InSAR geometric imaging disposition various approaches may be used to convert the unwrapped InSAR measured interferogram to the corresponding ground points on a pixel-by-pixel basis. A procedure for converting the unwrapped InSAR phase image to height values in a specific map projection system is described in Kenyi & Raggam (1996). This tool was modified to simulate interferograms in slant range geometry from a DEM in specific map projection (Figure 2).

The simulation interferogram was co-registered to that measured by InSAR to within pixel accuracy. Figure 3 shows a comparison of the ERS measured and simulated wrapped interferograms. The unwrapped (or absolute value) simulated interferogram was then used to remove the topographic component from the interferogram of the orbit pair 06279-05778. The removal was carried out in the complex domain by conjugating the simulated interferogram and multiplying it with that measured by InSAR. The residual interferogram is the D-InSAR product shown in Figure 4a. The D-InSAR interferogram was then smoothed to reduce

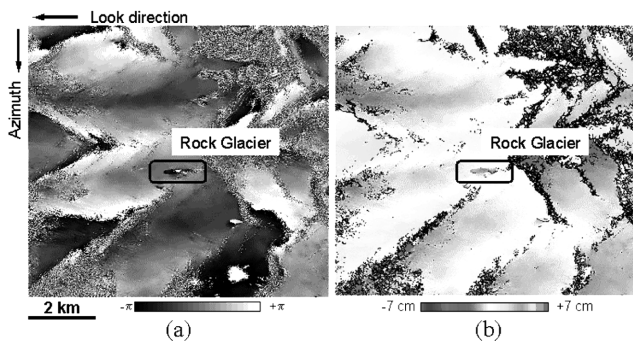


Figure 4. Difference interferogram generated by subtraction of topographic phase simulated from DEM and InSAR interferogram from ERS-1 orbit pair 06279-05778. Interferogram in (a) wrapped and (b) unwrapped and scaled.

speckle using spectral filtering (Goldstein & Werner 1998). The speckle filtered interferogram was phase unwrapped using the branch-cut method of Goldstein et al. (1988). The resulting unwrapped interferogram was then scaled to cm level to produce the radar line-of-sight displacement map shown in Figure 4b.

#### 4 QUANTITATIVE ANALYSIS

The quantitative analysis is based on the Doesen rock glacier area delineated in the box of Figure 4. The error in the analysis was estimated from the residuals in the non-moving areas at about  $\pm 1.4$  mm rms. The final result is shown in Figure 5a and presented as a displacement map with contour line intervals of 1.0 mm in ground range geometry. The areas with statistically insignificant displacements are coded gray, e.g. 2 times rms. For the other image pair combinations, coherency in the area where the rock glacier is located was too low for successful processing.

The image in Figure 5a clearly reveals the spatial distribution of the surface deformation of the rock glacier in the radar line-of-sight. The processes involved in the dynamics of rock glaciers are general mass advection, advection of topography by creep, 3-dimensional straining and local mass changes due to ice melt or refreezing (Kääb et al. 2003). For flow velocity measurement tracking is required. Thus, the flow velocity of rock glaciers cannot be deduced from D-InSAR displacement maps without preliminary assumptions of the various processes involved.

The maximum deformation (point A in Figure 5a) measured in the D-InSAR map was about  $-18$  mm/35 days and the changes at the snout of the rock glacier (point S in Figure 5a) amounted to  $-10$  mm/35 days. The overall mean deformation rate was about  $-6$  mm/35 days. The quantitative validation of these results with annual geodetic measurements and multi-year photogrammetric investigations (e.g. Kaufmann 1998) is not adequate, since the data were not taken at

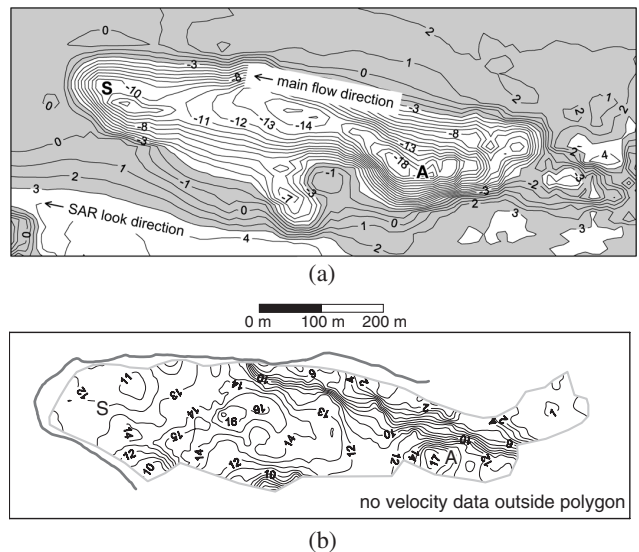


Figure 5. (a) Close-up of the area marked with a box in Figure 4b in isolines of 1 mm displacements for ERS cycle of 35 days with non-moving parts in gray. (b) Isolines of 1 cm of photogrammetrically derived mean annual horizontal flow velocity for the time period 1975-1993.

the same period and the measurements are not directly comparable.

The spatial distribution of the surface deformation is smooth however, which is also true for the photogrammetrically derived lines of equal horizontal flow velocity (Figure 5a with 5b). The obtained D-InSAR measurements, such as the observed surface deformation, must be attributed mainly to the vertical surface change as a result of the various processes mentioned above. Currently the dynamics of rock glaciers are not well understood. For this reason the International Permafrost Association (IPA) has setup a task force on Permafrost Creep and Rock Glacier Dynamics. The aim of this task force is to define the current level of knowledge with respect to the potential for numerically modelling the flow and evolution of perennially frozen ice/rock-mixtures.

In order to extract physically meaningful information from the D-InSAR measured surface deformation that could be attributed to specific processes, a complementary orbit would be useful. In an alpine environment however, the orientation of the rock glacier in respect to the radar line of sight does matter. In a best case scenario the rock glacier must be located in a back slope and the flow direction must be parallel to the radar line-of-sight, with only ascending or descending orbits being used.

#### 5 CONCLUSIONS

The detection and measurement of surface deformation of a small active rock glacier using ERS D-InSAR

data has been successfully demonstrated. The mean deformation rate of the rock glacier surface (in the radar line-of-sight) was estimated to be about  $-6$  mm/35 days. Because the deformation is complex and results from general mass advection, advection of topography by creep, 3-dimensional straining and local mass changes due to ice melt or refreezing, it is difficult to assign the D-InSAR results to specific components.

For a successful detection and quantification of rock glacier deformation in the Alps, InSAR data with very small normal baseline components and a multi-looking of 5 looks are required. The glacier must be located on a back slope (otherwise it will be a layover) and the flow must be in the SAR line-of-sight. The temporal baseline must be very short, and the period of August to September is the optimum time for InSAR data acquisition as at this time of the year the majority of the rock glacier is snow free. If this is not the case then the data will be temporally decorrelated.

As a result of the successful launch of ENVISAT and the upcoming spaceborne SAR missions, SAR data will be increasingly available during the coming decades. The proposed application of SAR interferometry for the world wide monitoring of rock glaciers can be further investigated and perhaps developed to a fully operational level.

#### ACKNOWLEDGMENT

The data used were provided by ESA as part of the ERS Tandem AO project no. AOT.A301. The financial support of the Hohe Tauern National Park is kindly appreciated.

#### REFERENCES

- Barsch, D. 1996. Rock glaciers: indicators for the present and former Geocology in high mountain environment. *Springer Series in Physical Environment* 16: 331.
- Gabriel, A.K., Goldstein, R.M. & Zebker, H.A. 1989. Mapping small elevation changes over large areas: Differential radar interferometry. *J. of Geophysical Research* 94(B7): 9183–9191.
- Goldstein, R.M., Zebker, H.A. & Werner, C.L. 1988. Satellite radar interferometry: Two-dimensional phase unwrapping. *Radio Science* 23(4): 713–720.
- Goldstein, R.M. & Werner, C.L. 1998. Radar interferogram filtering for geophysical applications. *Geophysical Research Letters* 25(21): 4035–4038.
- Kääb, A., Kaufmann, V. & Eiken, T. 2003. Rock glacier dynamics: implications from high-resolution measurements of surface velocity fields. *Proceedings of the 8th International Conference on Permafrost, Zurich, Switzerland* (this volume).
- Kaufmann, V. 1998. Deformation analysis of the Doesen rock glacier (Austria). *Proceedings of the 7th International Permafrost Conference, Yellowknife, Canada, Collection Nordicana* 57: 551–556.
- Kenji, L.W. & Raggam, H. 1996. Accuracy Assessment of Interferometrically Derived DTMs. *Proceedings of ESA FRINGE'96 Workshop on ERS SAR Interferometry, 30 September–2 October, Zurich, Switzerland*: 51–56.
- Kenji, L.W., Raggam, H. & Schardt, M. 1996. SAR Interferometry: Experiences with ERS-1/2 SLC Data. *The Austrian Journal of Survey & Geoinformation, VGI, special edition for the XVIIIth ISPRS-Congress 9–19 July, Vienna, Austria* 2(96): 157–164.
- Lieb, G.K. 1998. High-mountain permafrost in the Austrian Alps (Europe). *Proceedings of the 7th International Permafrost Conference, Yellowknife, Canada, Collection Nordicana* 57: 663–668.
- Massonet, D., Rossi, M., Carmona, C., Adragna, F., Peltzer, G., Feigl, K. & Rabaute, T. 1993. The displacement field of Landers earthquake mapped by radar interferometry. *Nature* 364: 138–142.
- Prati, C., Rocca, F. & Monti-Guarnieri, A. 1992. SAR interferometry experiments with ERS-1. *Proceedings of 1st ERS-1 Symposium, Cannes, France*: 211–218.
- Rott, H. & Siegel, A. 1999. Analysis of mass movements in alpine terrain by means of SAR interferometry. *Proceedings of IGARSS'99, 28 June–2 July, Hamburg, Germany*: 1933–1936.
- Wang, Z. & Li, S. 1999. Detection of winter frost heaving of the active layer of Arctic permafrost using SAR differential interferograms. *Proceedings of IGARSS'99, 28 June–2 July, Hamburg, Germany*: 1946–1948.
- Wegmueller, U. & Strozzi, T. 1998. Characterization of differential interferometry approaches. *Proceedings of EUSAR'98, 25–27 May, Friedrichshafen, Germany*: 237–240.
- Zebker, H., Werner, C., Rosen, P. & Hensley, S. 1994. Accuracy of topographic maps derived from ERS-1 interferometric radar. *IEEE Transaction on Geoscience and Remote Sensing* 32(4): 823–836.

